IJMF, Iranian Journal of Materials Forming, Vol. 2, No. 2, pp 14-26
Printed in The Islamic Republic of Iran, 2015

Effect of the particle size on the deformation and fracture behavior of Al/4vol.%Al_2O_3 composite produced by accumulative roll bonding (ARB)

M. Reihanian*, M. Naseri and M. Jalili Shahmansouri

Department of Materials Science and Engineering, Faculty of Engineering, Shahid Chamran University of Ahvaz, Ahvaz, Iran

Abstract: In this study, Al/Al_2O_3 composites with two different particle sizes of 1 µm and 0.3 µm were produced via accumulative roll bonding (ARB). The microstructure evolution, mechanical properties and fracture behavior of the composites were investigated. Results show that higher ARB cycles are required to achieve a uniform distribution of particles in the composite with 0.3 µm particle size. During ARB, dense cluster of the particles broke up and a uniform distribution of particles was achieved after eight ARB cycles. The tensile strength of the composite with 1 µm and 0.3 µm particle size enhanced by increasing the number of ARB cycles, reached to about 170MPa and 175MPa, respectively, in comparison to that of the annealed Al (about 47 MPa). The finer particles caused a higher tensile strength due to the decrease in the distance between the particles at a given volume fraction. The fracture surface of both composites revealed ductile type fracture characterized by dimples. It was shown that, the dimples in the composite with particle size of 1 µm were larger and deeper.

Keywords: Accumulative roll bonding (ARB), Metal matrix composites (MMCs), Microstructure, Mechanical properties

1. Introduction

Al alloys reinforced with ceramic particulates have significant potential for structural applications due to their high specific strength and stiffness as well as low density[1]. These properties have made Al-based metal matrix composites (MMCs) an attractive candidate for the use in weight-sensitive and stiffness-critical components in aerospace, transportation and industrial sectors [2]. The production methods of MMCs can be divided into two main categories: (a) solid state methods such as mechanical milling and powder metallurgy [3] and (b) liquid state methods such as stir casting [4]. The main problems in these methods are high-energy consumption and formation of defects such as porosity, particle agglomeration and particle free zones (PFZs). As a result, the mechanical properties of the composites may be reduced. In addition, since an expensive equipment is required and the processing routes are usually complex, the cost to produce MMCs by these methods is high. To overcome the aforementioned problems, accumulative roll bonding (ARB), as a severe plastic deformation (SPD) method, has been used as an effective method to fabricate MMCs such as in Refs. [5-8]. Briefly, ARB consists of multiple cycles of surface preparation, stacking, rolling (50% reduction in thickness) and cutting of the metal strips [9]. During ARB, large plastic strains are imposed into the material without a significant change in the cross section to fabricate ultrafine-grained metals with superior mechanical properties [10]. Combining the strengthening mechanisms including strain hardening, grain refinement and the second phase particles in the ARB-processed MMCs, leads to the production of high-strength Al-based composites.

At present, a wide variety of MMCs with different type of reinforcements has been made by ARB. For example, Jamaati et al. [11] and Rezayat et al. [12] have fabricated the particulate Al/Al_2O_3

Received by the editors July 3, 2015; Revised July 27, 2015 and Accepted August 6, 2015.
*Corresponding author (reihanian@scu.ac.ir)

composites by ARB process. However, only a slight attempt has been made to investigate the effect of particle size on the mechanical behavior and microstructure of MMCs produced by ARB. Jamaati et al. [13] have investigated the effect of SiC particle size on microstructure and mechanical properties of Al/10vol.%SiC composite produced by ARB. They found that the microstructure of the composite with larger particle size becomes uniform more rapidly with high bonding quality and without any porosity, compared to the composite with smaller particle size. They also found that the tensile strength of both composite improved with increasing the number of ARB cycles. Karbalaei Akbari et al. [14] studied the effects of particle size/volume fraction of TiB_2 particles on the microstructure and mechanical properties of A356/TiB_2 nano- and micro-composite. They found that the porosity content of the composites increased with increasing the volume fraction and decreasing the particle size of ceramic reinforcements. Their results demonstrated that a significant improvement in tensile strength and elongation was attained in the 1.5 vol.% TiB_2 composite, compared with a non-reinforced alloy nano-composite while further increase in TiB_2 nanoparticle content led to reduction in strength values and elongation of nano-composites.

Up to now, the effect of alumina size on the microstructure and mechanical properties of the produced composites has not been studied. The aim of this work is to fabricate Al/4vol.%Al_2O_3 composites by ARB process and to investigate the effect of the alumina size on the mechanical properties and fracture of the produced composite. In the literature, the amount of the reinforcement is based on the volume fraction and usually is in the range of 2-15 vol.% [11, 12, 15-17]. Thus, in the present study, the volume fraction of 4% is considered as a typical for the two particle sizes.

2. Materials and methods

As-received strips of commercial pure Al with 150 mm long, 50 mm wide, and 0.9 mm thick, annealed at 673 K for 2 h, and Al_2O_3 particles with two different average sizes of 1 and 0.3 μm were used as raw materials (Fig. 1). The chemical composition of aluminum alloy used in this study is shown in Table 1. The principle of ARB process to fabricate MMCs is schematically shown in Fig. 2.

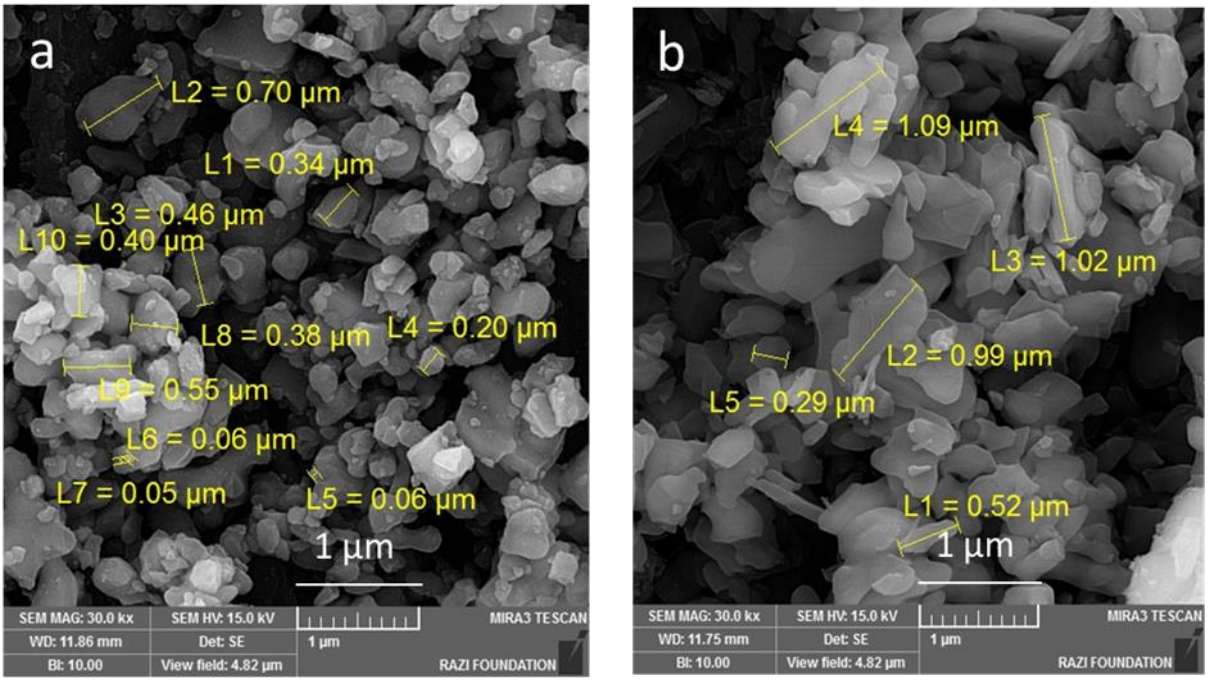

Fig. 1. SEM images of the Al_2O_3 particles with the average size of about (a) 0.3 μm and (b) 1 μm.

Table 1.Chemical composition (wt.%) of aluminum strips.

Al (99.7)									
Si	Fe	Cu	Mn	Mg	Zn	Cr	Ni	Ti	Be
0.0487	0.200	0.0058	<0.001	<0.0001	<0.005	<0.001	<0.005	0.0097	<0.0001
Ca	Li	Pb	Sn	Sr	V	Na	Bi	Zr	B
<0.0005	<0.0001	<0.002	0.0019	<0.0001	0.0115	0.0035	<0.005	<0.002	<0.0005
Ga	Cd	Co	Ag	Hg	In				
0.0079	<0.001	<0.003	<0.001	<0.003	<0.01				

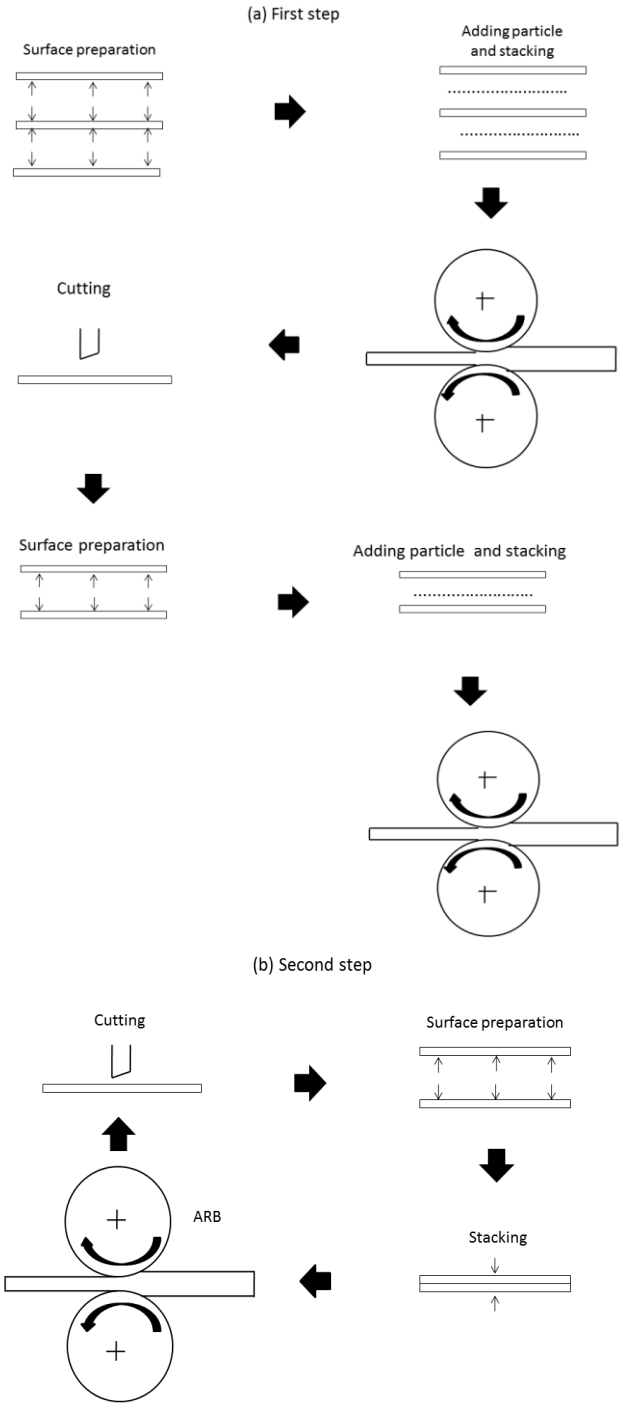

Fig. 2. Schematic illustration of ARB process for fabrication of Al/Al_2O_3 composites; (a) the first and (b) the second step.

The Al/Al_2O_3 composite was fabricated in two steps. In the first step, three annealed strips were surface prepared by degreasing in acetone bath and then scratch brushing with wires of 0.3 mm in diameter. An appropriate 2 vol.% of Al_2O_3 particles was uniformly dispersed between them and stacked tightly at the edges. The roll-bonding process was carried out with a specific amount of reduction equal to 50%. Then, the roll-bonded strip was cut into two parts with the same dimensions. Following the preparation of the surfaces, the sectioned-strips were stacked and roll-bonded again under the same conditions as the first cycle, while the remaining 2 vol.% of Al_2O_3 particles dispersed between them. After this step, the total amount of Al_2O_3 particles reached to 4 vol.% and the thickness of the composite sheet was about 1.35 mm. The total volume of Al strips is $3\times(15\times5\times0.09)=20.25cm^3$. To have a 0.04 volume fraction of the particles, the total volume of particles must be $0.04\times20.25=0.81cm^3$. Considering the density of alumina (3.95 g/cm^3), the total amount of the particle to have a 0.04 volume fraction is determined as $3.95\times0.81=3.2\,g$. This amount was added between the Al strips in the first step of the process. The particles were added by using a sieve with a mesh somewhat larger than the particle size. For this purpose, the particles were poured on the sieve and then dispersed manually on the surface of the strip. It is noted that at this stage (the first step), the distribution of the particles are not uniform. In the second step, the strips were cut, surface prepared, stacked and roll bonded (50% reduction) without adding the particles between the layers. This step was repeated up to six cycles and designed to remove the particles from the layer interfaces and to distribute the particles in the matrix. The roll-bonding process was carried out without lubrication, using a laboratory rolling mill with a loading capacity of 35 tons. The roll diameters were 170 mm, and the rolling speed was set at 10 rpm.

The microstructural observation and fracture surface of the specimens was evaluated by a MIRA3 TESCAN scanning electron microscope (SEM) equipped with energy dispersive spectroscopy (EDS). SEM analysis was examined on the rolling direction-normal direction (RD-ND) and rolling direction-transverse direction (RD-TD). The samples were sectioned by a micro-cutter and mounted by a conductive material under the heat and high pressure. The mounted samples were ground by relatively fine abrasive papers and polished subsequently by clothes and diamond pastes without using the etching process. Tensile test was done at room temperature with a tensile testing machine (SANTAM STM-150) under a nominal initial strain rate of $10^{-3}s^{-1}$. The tensile test specimens were machined from the ARBed strips oriented along the rolling direction according to the ISO 6892 (No.3). The gage width and length of the samples were 5 and 10 mm, respectively. For each cycle, two tensile samples were provided. It is noticed that the number of tensile samples prepared from the ARB sheets was limited due to edge cracking and trimming after each cycle. Since the result of the test was approximately the same for each cycle, only one of them was selected as a typical.

3. Results and discussion

3.1. Microstructure observation

SEM micrographs of Al/Al_2O_3 composite with 1 μm particle size at the RD-ND plane after various ARB cycles are shown in Fig. 3. It can be seen that after the two cycles (Fig. 3a), there is 4 layers of Al_2O_3 particles between 6 layers of Aluminum strips. After four (Fig. 3b) and six (Fig. 3c) cycles, the composite should contain 24 Al and 16 Al_2O_3 layers and 96 Al and 64 Al_2O_3 layers, respectively. However, as the interface between different layers is not identifiable anymore, it is very difficult to recognize the number of layers in the micrograph. After eight cycles of ARB process (Fig. 3d), the composite strip should contain 384 Aluminum and 256 Al_2O_3 layers. It is emphasized that the low magnification SEM image (Fig. 3) is not used to prove the bonding quality of the particles with the Al matrix. This figure is just provided to show the increase in the layer numbers and to explain the fragmentation of the interfaces where the alumina particles are present. This is particularly evident after eight ARB cycles (Fig. 3d) in

which the particles at interfaces are broken into small fragments, showing the discontinuity at the interfaces and distribution of the alumina particles at the RD-ND plane.

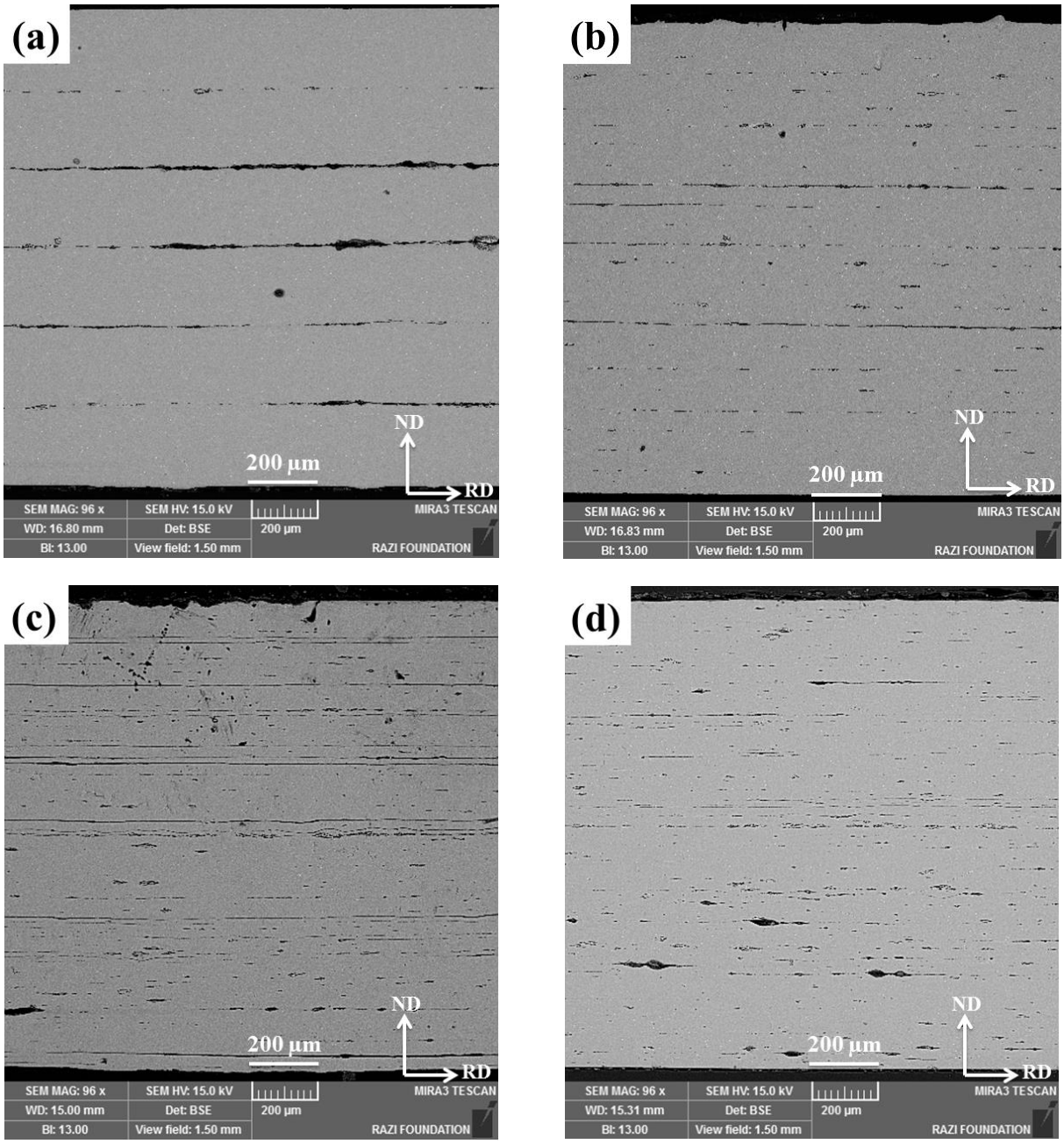

Fig. 3. SEM micrographs of the Al/Al_2O_3 composite with particle size of 1 µm at the RD-ND plane after (a) two, (b) four, (c) six, and (d) eight ARB cycles.

The major mechanism at low temperature deformations can be explained by film theory [18]. According to this mechanism, the extrusion of virgin metal through the cracks has the major role in the real contact between metals. In the case of the particulate MMCs, it has been reported that ceramic particles can act as barriers to film theory and inhibit the creation of good bonding [19]. However, the rolling pressure supplies sufficient force and can create large contact areas. Therefore, good bonding can be achieved at high ARB cycles even in the presence of ceramic particles.

SEM images of the Al/Al_2O_3 composite with 0.3 µm particle size at the RD-ND plane after various ARB cycles are shown in Fig. 4. A similar trend for the evolution of the microstructure is observed for this

composite. However, in contrast to the composite with 1 μm particle, several interfaces remain adherent even at high ARB cycles (after six and eight cycles). In other words, higher ARB cycles are required to disintegrate the interfaces and to distribute the alumina particles at the RD-ND plane. This can be explained by the model developed recently by Reihanian et al. [20]. According to this model, the critical reduction, R_{cr}, needed to achieve a uniform distribution of particles in particulate MMCs depends on the particle size, d, volume fraction, f, and the initial thickness of the strips, $t_\circ$, as below[20]:

$$R_{cr} = 1 - \left[\frac{\sqrt{3}\pi}{8f}\right]^{1/3}\left(\frac{d}{t_\circ}\right) \quad (1)$$

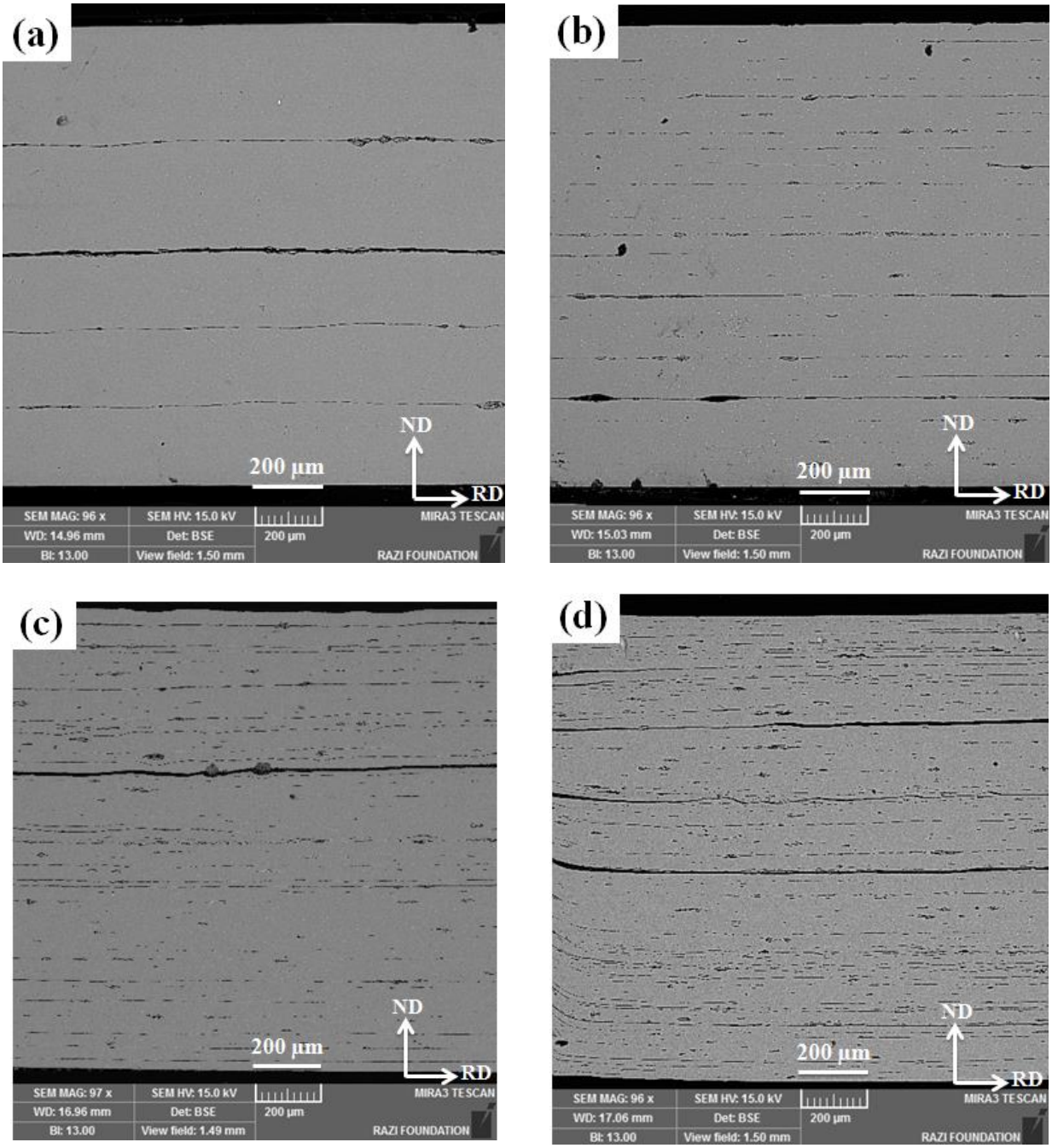

Fig.4. SEM micrographs of the Al/Al_2O_3 composite with particle size of 0.3 μm at the RD-ND plane after (a) two, (b) four, (c) six and (d) eight ARB cycles.

For, $f = 0.04$, $t_\circ = 0.9\,mm$, $d_1 = 1\,\mu m$ and $d_2 = 0.3\,\mu m$, the critical reduction is predicted as 0.9971 and 0.9991, corresponding to the effective strains of 6.7 and 8.1, respectively, while a total effective strain of 6.4 is imposed after eight ARB cycles. The strain imposed after eight ARB cycles (6.4) is relatively lower than the predicted value of the composite with 0.3 μm particle size (8.1). It means that at least 11 ARB cycles are required to get a uniform distribution of particles in this composite. Since the material is work hardened and its strength increases remarkably during ARB, it is somewhat difficult experimentally to reach to this high level of ARB process. On the other hands, the critical strain imposed after eight ARB cycles (6.4) is approximately comparable to the predicted value of the composite with 1 μm particle size (6.7). Therefore, a uniform distribution of particles is rather expected in this composite and the microstructure of the composite with particle size of 1 μm is investigated experimentally in detail (Figs. 5 and 6) as typical.

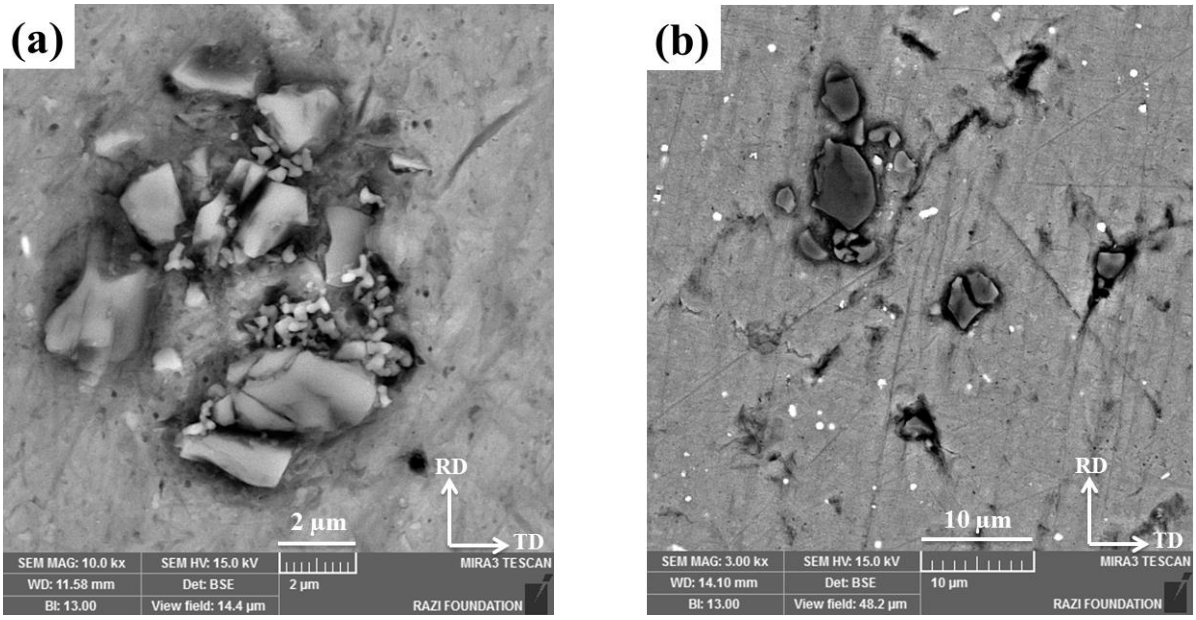

Fig. 5. SEM micrographs of the Al/Al_2O_3 composite with particle size of 1 μm after: (a) two and (b) eight ARB cycles showing the clustering and de-clustering of the particles.

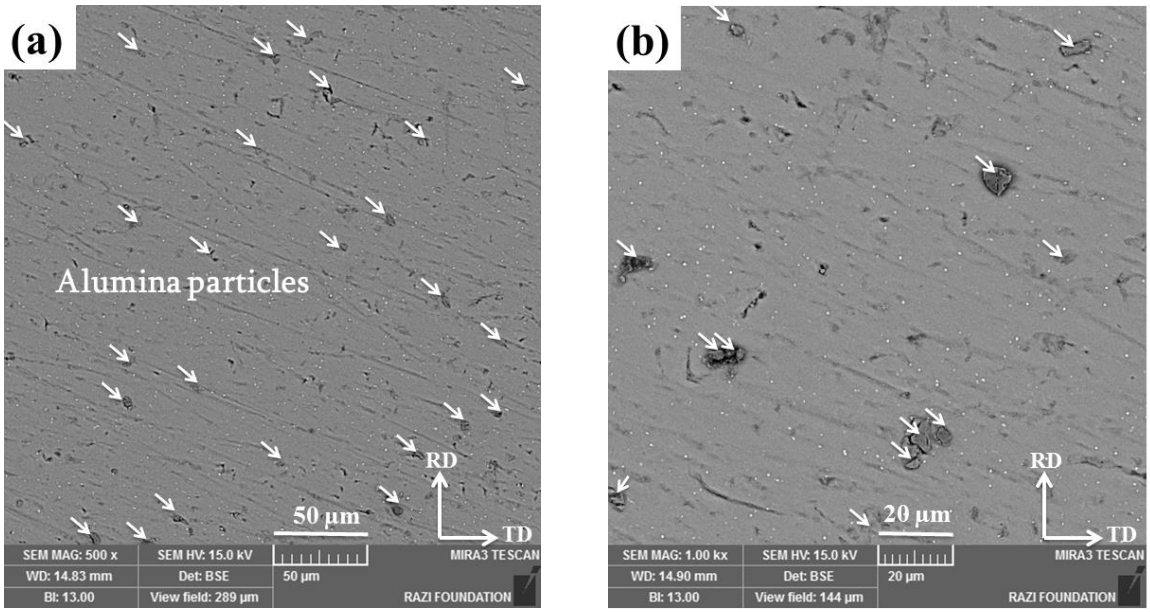

Fig. 6. SEM images of the Al/Al_2O_3 composite with particle size of 1 μm after the eight ARB cycles at (a) low and (b) high magnification showing the distribution of the alumina particles.

Figure 5 shows typical SEM micrographs of the Al/Al_2O_3 composite with 1 μm particle at higher magnifications after two and eight ARB cycles. It is seen that, after two ARB cycles, several Al_2O_3 particles are clustered and agglomerated by each other (Fig. 5a). Agglomeration and clustering of the Al_2O_3 particles can be induced by their attractive Van der Waals interactions of Al_2O_3 particles coupled with their large surface-to-volume ratio. This is occurred when the Al_2O_3 particles are added between the strips in the first step of ARB process. However, the distribution of the Al_2O_3 particles in the Al matrix is improved by increasing the number of ARB cycles. As the ARB proceeds, the number of the Al_2O_3 particles that are involved in each cluster, decreases to some extent (Fig. 5b). As a result, a uniform distribution of particles is fairly achieved at last stages of ARB. To investigate the distribution of the Al_2O_3 particles, typical SEM micrographs at the RD-TD plane of the Al/Al_2O_3 composite after eight ARB cycles are shown in Fig. 6. It is clear that the distribution of Al_2O_3 particles in the Al matrix is uniform after eight cycles. During ARB, the Al matrix is extruded and flows through clusters of the Al_2O_3 particles. Therefore, dense clusters can be modified to diffuse ones, and the distance between the particles constituting the clusters is enhanced [21]. In addition, cluster of the particles are elongated in the rolling direction [22]. As a result, the distance between the particles increases and the distribution of the particles improves within the Al matrix.

3.2. Mechanical Properties

The engineering stress–strain curves of the annealed as well as Al/Al_2O_3 composites with 1 μm and 0.3 μm particle size after six and eight ARB cycles are presented in Fig. 7. It is observed that the tensile strength increases with increasing the number of cycles. After eight cycles, the composite with 1 μm and 0.3 μm particle size exhibits the tensile strength of about 170 MPa and 175 MPa, respectively, compared with the annealed Al (About 47 MPa). According to the previous work [7], the tensile strength of the pure Al, after eight ARB cycles, reaches to about 150 MPa. The tensile strength of the Al/Al_2O_3 composite with 1 μm and 0.3 μm particle size is about 3.6 and 3.7 times higher than that of the annealed Al, respectively. It has been reported that the variations in the tensile strength of the ARB-processed materials is due to the strain hardening (dislocation strengthening), the evolution of the grain structure and the formation of ultra-fine grains (grain boundary strengthening mechanism). In the early stages of ARB process, strain hardening acts as the main strengthening mechanism while at last stages, grain refinement has the major role [23, 24]. The increase in dislocation density within the grains or formation of low angle dislocation boundaries are the main reasons of strain hardening in SPD processed materials [23]. As the effect of work hardening decreases, gradual evolution of ultra-fine grains plays the main role in strengthening. During SPD processing, the misorientation of the dislocation boundaries increases gradually while their sizes decreases. At final stages, a large fraction of low angle grain boundaries changed into high angle ones and grain refinement to the ultra-fine scale causes the increase in the strength [24]. In the case of the particulate MMCs, other strengthening mechanism such as Orowan looping [25] can contribute to the strength of the composite. In this mechanism, the dislocations extrude between the particles leaving dislocation loops around them. Orowan looping causes the mean distance between the particles to decrease and the stress required for movement of subsequent dislocations to increase. The activation of the further (secondary) slip systems at the interfaces [26, 27] and the difference in the thermal expansion coefficient of the metal constituents [13] have additional contribution through generation of new dislocations.

Regarding Fig. 7, the tensile strength of the composite containing 1 μm particle sizeis slightly lower compared to that of the composite with 0.3 μm particle size. Similar results have been reported in literature where the effect of the particle size is investigated [13, 14]. Since the volume fraction of the particles in both composites is the same, therefore, the matrix/particle interface of composite with 0.3 μm

particle size is more than that of the composite with 1 μm particle size. The finer particles leads to a higher tensile strength due to the decrease in the distance between the particles at a given volume fraction.

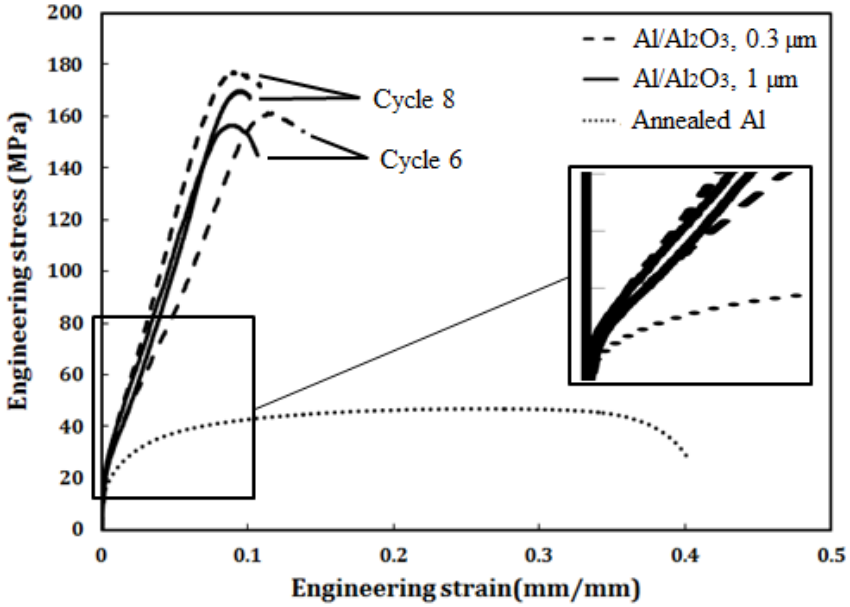

Fig. 7. Engineering stress–strain curves of the annealed Al and the Al/Al_2O_3 composites with particle sizes of 0.3 μm and 1 μm.

The elongation of the composites after six and eight cycles is about 10%, which show a remarkable decrease in comparison to that of the annealed Al (about 40%). The sharp decrease in the elongation is the characteristics of each SPD process [28] and can be attributed to the large increase in dislocation density and the accumulation of internal stresses that promote the nucleation of cracks. It is noted that the composites with 1 μm and 0.3 μm particle size approximately exhibit similar values of the elongation. Nevertheless, to compare the elongation of these composites, the precise value of the elongation needs to be measured. This can be obtained by using the extensometer during the tensile test, which is somewhat difficult in practice because the gage length of the ARB processed materials is relatively small.

In general, the tensile test is not an appropriate tool to analyze the elastic properties of the materials and more accurate test methods are required. Therefore, the engineering stress-strain curves do not exhibit a significant difference between the elastic modulus of the composites and the pure Al. A similar trend can also be observed in literature such as in Al/SiC [5], Al/B_4C [16, 27], Al/Cu_P [29] and Al/Al_2O_3/SiC hybrid composite [30].

3.3. Fractography

Figure 8 illustrates SEM fractographs of the fracture surface of tensile test specimens for the Al/Al_2O_3 composites with 1 μm and 0.3 μm particle size after eight ARB cycles. The fracture surface of both composite shows a typical ductile fracture that is characterized by dimples. The presence of dimples and gray fibrous appearance are the characteristics of the most metals with ductile tensile fractures [25]. This type of fracture arises due to the nucleation of microvoids at the head of the cracks or locked dislocations and consequent coalescence of the voids. These voids can be elongated in one direction due to unequal triaxial stresses [31]. It has been reported that the state of stress can affect the shape of the dimples [32]. In the presence of tensile stresses, the shape of the dimples is equiaxed while they become elongated in one direction when the state of stress is shear as reported previously in the hybrid composite [30]. Figure 8 shows that the failure mode of composites is tensile ductile rupture. It is clearly observed that the particle

size affects the size and depth of the dimples. The Al/Al_2O_3 composite with particle size of 1 μm revealed larger and deeper dimples (Fig. 8a and b) in comparison to the Al/Al_2O_3 composite with particle size of 0.3 μm (Fig. 8c and d). The presence of the particles can transform the appearance of fracture surface of the composites so that the dimples nucleated at the particle sites become deeper and larger than the dimples nucleated in another regions. The presence of particles at the bottom of some dimples is indicated by arrows and can be the evidence of void nucleation from particle/matrix interfaces. This is particularly obvious in Fig. 8b where several small dimples are observed around the larger ones. The EDS results at the exhibited points A and B (Fig. 8e and f) confirmed the presence of the alumina particles at the bottom of the dimples. In general, several factors such as size, type, shape, volume fraction, aspect ratio, distribution of particles and interface properties can affect the fracture properties of a particulate composite. The effect of these parameters on the fracture behavior of the particulate MMCs needs to be investigated independently. In the present study, only the effect of particle size is evaluated.

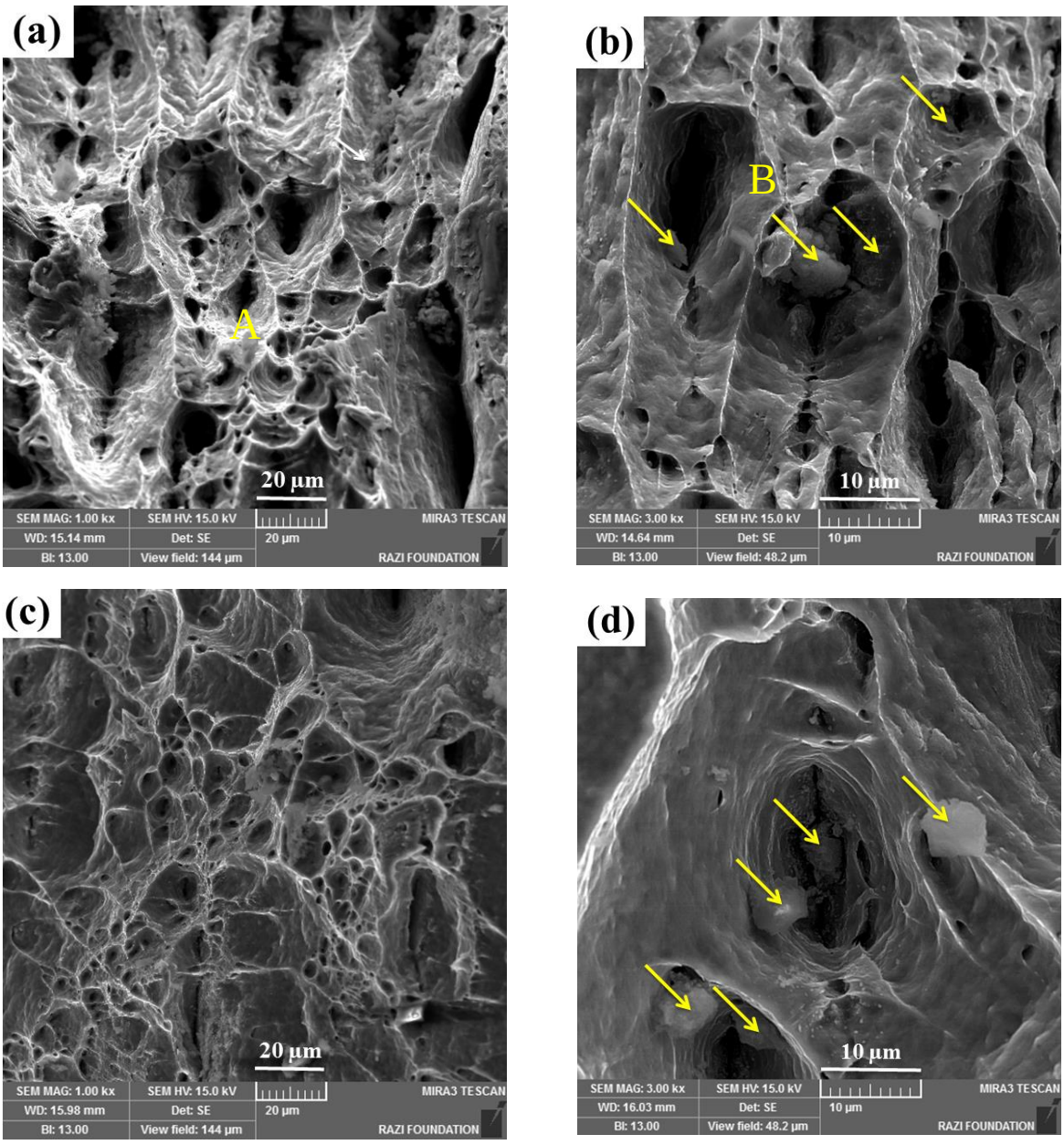

Fig. 8. Tensile fracture surface of Al/Al_2O_3 composite with (a) and (b) 1 μm and (c) and (d) with 0.3 μm particle size after eight ARB cycles; (e) and (f) the EDS results at the point A and B, respectively.

Figure 8 continued.

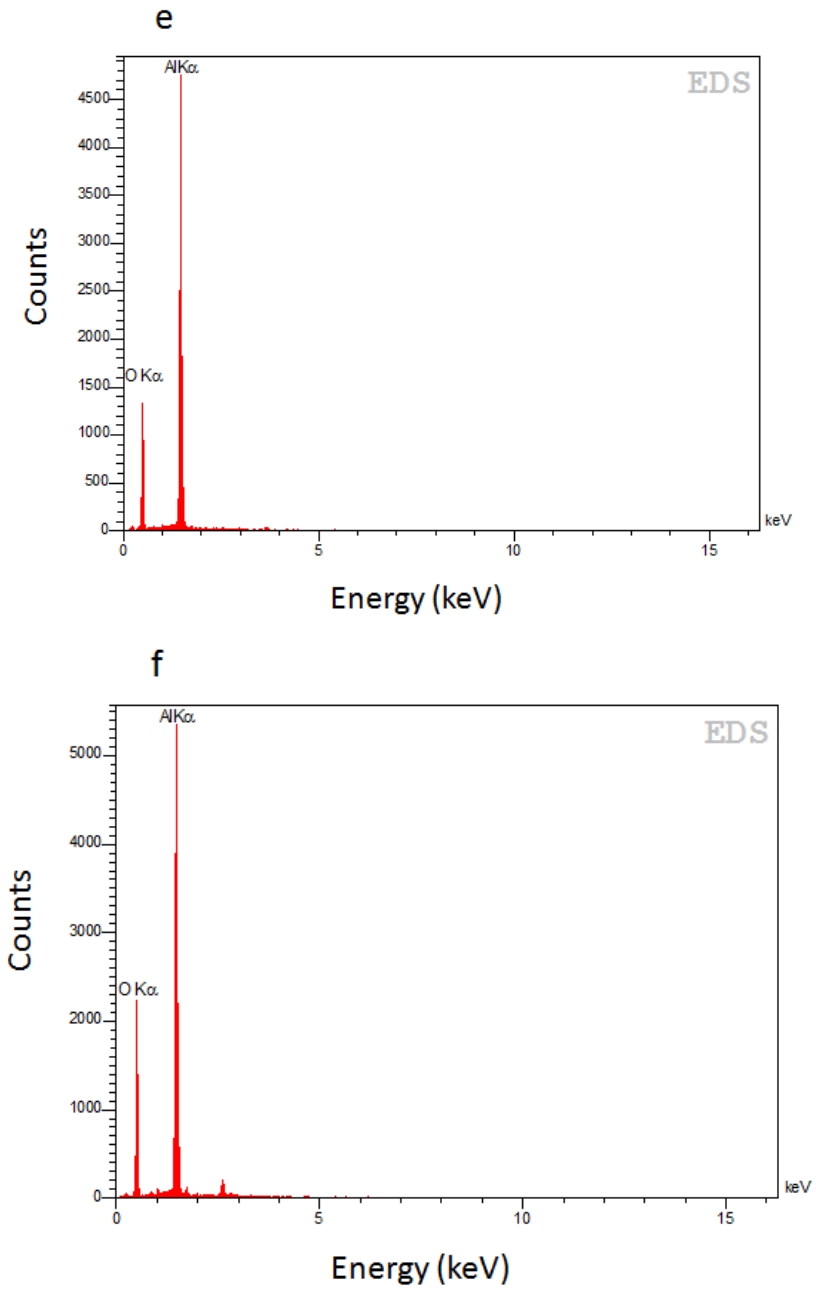

4. Conclusion

1. The ARB process was successfully used to fabricate the Al/4vol.%Al_2O_3 composites with two different particle sizes of 1 μm and 0.3 μm.
2. The Al/Al_2O_3 composite with particle size of 1 μm reveals a rather uniform distribution of particles after eight ARB cycles.
3. During ARB, dense cluster of the particles breaks and splits into the diffuse ones involving only a small number of particles.
3. The Al/Al_2O_3 composite with 1 μm and 0.3 μm particle size exhibits a much higher tensile strength (170 and 175 MPa, respectively) compared with that of the annealed Al (47 MPa). The higher strength of the Al/Al_2O_3 composite with 0.3 μm particle size is attributed to its higher matrix/particle interface.

4. The fracture surface of Al/Al_2O_3 composite indicates the ductile fracture mode characterized by dimples. The Al/Al_2O_3 composite with the particle size of 1 μm revealed larger and deeper dimples in comparison to the Al/Al_2O_3 composite with particle size of 0.3 μm.

Acknowledgments: The financial support of Shahid Chamran University of Ahvaz through the Grant number 93-02-27171 is appreciated.

5. References

[1] D.B. Miracle, Metal matrix composites–From science to technological significance, *Composites Science and Technology*, 65(2005) 2526-2540.

[2] D.J. Lloyd, Particle reinforced aluminium and magnesium matrix composites, *International Materials Reviews*, 39(1994) 1-23.

[3] G. O'Donnell and L. Looney, Production of aluminium matrix composite components using conventional PM technology, *Materials Science and Engineering: A*, 303(2001) 292-301.

[4] J. Hashim, L. Looney and M.S.J. Hashmi, Metal matrix composites: production by the stir casting method, *Journal of Materials Processing Technology*, 92–93(1999) 1-7.

[5] M. Alizadeh and M.H. Paydar, Fabrication of nanostructure Al/SiC_P composite by accumulative roll-bonding (ARB) process, Journal of Alloys and Compounds, 492 (2010) 231-235.

[6] R. Jamaati and M.R. Toroghinejad, Application of ARB process for manufacturing high-strength, finely dispersed and highly uniform Cu/Al_2O_3 composite, *Materials Science and Engineering: A*, 527(2010) 7430-7435.

[7] M. Reihanian, F.K. Hadadian and M.H. Paydar, Fabrication of Al–2vol% Al_2O_3/SiC hybrid composite via accumulative roll bonding (ARB): An investigation of the microstructure and mechanical properties, *Materials Science and Engineering: A*, 607(2014) 188-196.

[8] R. Jamaati, M.R. Toroghinejad and H. Edris, Effect of SiC nanoparticles on the mechanical properties of steel-based nanocomposite produced by accumulative roll bonding process, *Materials and Design*, 54(2014) 168-173.

[9] Y. Saito, H. Utsunomiya, N. Tsuji and T. Sakai, Novel ultra-high straining process for bulk materials—development of the accumulative roll-bonding (ARB) process, *Acta Materialia*, 47 (1999) 579-583.

[10] B.L. Li, N. Tsuji and N. Kamikawa, Microstructure homogeneity in various metallic materials heavily deformed by accumulative roll-bonding, *Materials Science and Engineering: A*, 423 (2006) 331-342.

[11] R. Jamaati and M.R. Toroghinejad, Manufacturing of high-strength aluminum/alumina composite by accumulative roll bonding, *Materials Science and Engineering: A*, 527(2010) 4146-4151.

[12] M. Rezayat, A. Akbarzadeh and A. Owhadi, Production of high strength $Al–Al_2O_3$ composite by accumulative roll bonding, *Composites Part A: Applied Science and Manufacturing*, 43 (2012) 261-267.

[13] R. Jamaati, S. Amirkhanlou, M.R. Toroghinejad and B. Niroumand, Effect of particle size on microstructure and mechanical properties of composites produced by ARB process, *Materials Science and Engineering: A*, 528(2011) 2143-2148.

[14] M. Karbalaei Akbari, H.R. Baharvandi and K. Shirvanimoghaddam, Tensile and fracture behavior of nano/micro TiB_2 particle reinforced casting A356 aluminum alloy composites, *Materials and Design*, 66(2015) 150-161.

[15] M. Alizadeh & M.H. Paydar, Fabrication of Al/SiC_P composite strips by repeated roll-bonding (RRB) process, *Journal of Alloys and Compounds*, 477(2009) 811-816.

[16] M. Alizadeh, Comparison of nanostructured Al/B4C composite produced by ARB and Al/B_4C composite produced by RRB process, *Materials Science and Engineering: A*, 528(2010) 578-582.

[17] A. Yazdani, E. Salahinejad, J. Moradgholi and M. Hosseini, A new consideration on reinforcement distribution in the different planes of nanostructured metal matrix composite sheets prepared by accumulative roll bonding (ARB), *Journal of Alloys and Compounds*, 509 (2011) 9562-9564.

[18] L. Li, K. Nagai and F. Yin, Progress in cold roll bonding of metals, *Science and Technology of Advanced Materials*, 9(2008) 023001.

[19] M. Alizadeh and M.H. Paydar, High-strength nanostructured Al/B_4C composite processed by cross-roll accumulative roll bonding, *Materials Science and Engineering: A*, 538(2012) 14-19.

[20] M. Reihanian, E. Bagherpour and M.H. Paydar, On the achievement of uniform particle distribution in metal matrix composites fabricated by accumulative roll bonding, *Materials Letters*, 91(2013) 59-62.

[21] M. Alizadeh, H.A. beni, M. Ghaffari and R. Amini, Properties of high specific strength Al–4wt.% Al_2O_3/B_4C nano-composite produced by accumulative roll bonding process, *Materials and Design*, 50(2013) 427-432.

[22] M. Rezayat, A. Akbarzadeh and A. Owhadi, Fabrication of high-strength Al/SiC_p nanocomposite sheets by accumulative roll bonding, *Metall and Mat Trans A*, 43(2012) 2085-2093.

[23] M. Reihanian, R. Ebrahimi, N. Tsuji and M.M. Moshksar, Analysis of the mechanical properties and deformation behavior of nanostructured commercially pure Al processed by equal channel angular pressing (ECAP), *Materials Science and Engineering: A*, 473(2008) 189-194.

[24] M. Reihanian, R. Ebrahimi, M.M. Moshksar, D. Terada and N. Tsuji, Microstructure quantification and correlation with flow stress of ultrafine grained commercially pure Al fabricated by equal channel angular pressing (ECAP), Materials Characterization, 59(2008) 1312-1323.

[25] T.H. Courtney, *Mechanical behavior of materials*, 2nd edition, Waveland Press, Inc., 2005.

[26] H. Sekine and R. Chent, A combined microstructure strengthening analysis of SiC_p/Al metal matrix composites, *Composites*, 26(1995) 183-188.

[27] M. Alizadeh, Strengthening mechanisms in particulate Al/B_4C composites produced by repeated roll bonding process, *Journal of Alloys and Compounds*, 509(2011) 2243-2247.

[28] A. Azushima, R. Kopp, A. Korhonen, D.Y. Yang, F. Micari, G.D. Lahoti, P. Groche, J. Yanagimoto, N. Tsuji, A. Rosochowski and A. Yanagida, Severe plastic deformation (SPD) processes for metals, *CIRP Annals - Manufacturing Technology*, 57(2008) 716-735.

[29] M. Alizadeh and M. Talebian, Fabrication of Al/Cu_p composite by accumulative roll bonding process and investigation of mechanical properties, *Materials Science and Engineering: A*, 558(2012) 331-337.

[30] A. Ahmadi, M.R. Toroghinejad and A. Najafizadeh, Evaluation of microstructure and mechanical properties of Al/Al_2O_3/SiC hybrid composite fabricated by accumulative roll bonding process, *Materials and Design*, 53(2014) 13-19.

[31] M.A. Meyers and K.K. Chawla, *Mechanical Behavior of Materials*, 2nd edition, Cambridge University Press, UK, (2009).

[32] D.J. Wulpi, *Understanding how Components Fail*, 3rd edition, ASM International, USA, (2013).